Synergistic Use of MODIS and AIRS in a Variational Retrieval of Cloud Parameters

JUN LI,* W. PAUL MENZEL,+ WENJIAN ZHANG,# FENGYING SUN,* TIMOTHY J. SCHMIT,+ JAMES J. GURKA,@ AND ELISABETH WEISZ*

*Cooperative Institute for Meteorological Satellite Studies, Space Science and Engineering Center, University of Wisconsin—Madison, Madison, Wisconsin
+Office of Research and Applications, NOAA/NESDIS, Madison, Wisconsin
#National Satellite Meteorological Center, Beijing, China
@Office of System Development, NOAA/NESDIS, Silver Spring, Maryland

(Manuscript received 13 October 2003, in final form 2 April 2004)

ABSTRACT

The Moderate Resolution Imaging Spectroradiometer (MODIS) and the Atmospheric Infrared Sounder (AIRS) measurements from the Earth Observing System's (EOS's) *Aqua* satellite enable global monitoring of the distribution of clouds. MODIS is able to provide a cloud mask, surface and cloud types, cloud phase, cloud-top pressure (CTP), effective cloud amount (ECA), cloud particle size, and cloud optical thickness at high spatial resolution (1–5 km). The combined MODIS–AIRS system offers the opportunity for improved cloud products, better than from either system alone; this improvement is demonstrated in this paper with both simulated and real radiances. A one-dimensional variational (1DVAR) methodology is used to retrieve the CTP and ECA from AIRS longwave (650–790 cm^{-1} or 15.38–12.65 μm) cloudy radiance measurements (hereinafter referred to as MODIS–AIRS 1DVAR). The MODIS–AIRS 1DVAR cloud properties show significant improvement over the MODIS-alone cloud properties and slight improvement over AIRS-alone cloud properties in a simulation study, while MODIS–AIRS 1DVAR is much more computationally efficient than the AIRS-alone 1DVAR; comparisons with radiosonde observations show that CTPs improve by 10–40 hPa for MODIS–AIRS CTPs over those from MODIS alone. The 1DVAR approach is applied to process the AIRS longwave cloudy radiance measurements; results are compared with MODIS and Geostationary Operational Environmental Satellite sounder cloud products. Data from ground-based instrumentation at the Atmospheric Radiation Measurement Program Cloud and Radiation Test Bed in Oklahoma are used for validation; results show that MODIS–AIRS improves the MODIS CTP, especially in low-level clouds. The operational use of a high-spatial-resolution imager, along with information from a high-spectral-resolution sounder will be possible with instruments planned for the next-generation geostationary operational instruments.

1. Introduction

Clouds play an important role in the earth's water and energy budgets. Their impact on the radiation budget can result in a heating or a cooling of the planet, depending on the radiative properties of the cloud and its altitude (Stephens and Webster 1981; Stephens et al. 1990). Cloud parameters, such as cloud-top height and fractional cloud coverage and emissivity, are useful in numerical weather prediction (NWP; Diak et al. 1998; Bayler et al. 2000; Kim and Benjamin 2000).

Many schemes have been proposed for estimating cloud parameters from multispectral radiance observations (Isaacs et al. 1986; Wielicki and Coakley 1981; Susskind et al. 1987; Eyre and Menzel 1989). One important method using passive remote sensing data for obtaining the altitude of mid- and upper-level clouds, especially transmissive clouds, is the CO_2-slicing technique (Chahine 1974; Smith et al. 1974; Smith and Platt 1978; Menzel et al. 1983; Menzel et al. 1992). Through satellite infrared remote sensing, cloud properties can be measured with high spatial and temporal resolution. The Geostationary Operational Environmental Satellite (GOES; Menzel and Purdom 1994) sounder cloudy radiance measurements, for example, provide hourly cloud parameters with a 10-km resolution (Schreiner et al. 2001).

The CO_2-slicing algorithm calculates both cloud-top pressure (CTP) and effective cloud emissivity or effective cloud amount (ECA; the product of the fractional cloud cover N and the cloud emissivity ε_c) from radiative transfer principles. This method takes advantage of the fact that each of the longwave infrared sounding spectral bands is sensitive to a different layer in the atmosphere. The CO_2-slicing technique has been shown to be effective for inferring cloud properties from broadband (with spectral resolution worse than 10 cm^{-1}) ra-

Corresponding author address: Dr. Jun Li, Cooperative Institute for Meteorological Satellite Studies, SSEC, University of Wisconsin—Madison, 1225 West Dayton Street, Madison, WI 53706.
E-mail: Jun.Li@ssec.wisc.edu

diance measurements for single-layer, nonopaque mid- to high-level clouds, such as cirrus (Baum and Wielicki 1994). The CO_2-slicing technique uses two spectral bands to obtain a solution (the spectral band pair depends on the cloud altitude); errors can be large in some atmospheric conditions, such as in the presence of a low-level temperature inversion, low clouds, and multilayer clouds. The accuracy of the CO_2-slicing cloud-top height and the sources of errors have been documented (Wielicki and Coakley 1981; Eyre and Menzel 1989; Wylie and Menzel 1989; Menzel et al. 1992; Schreiner et al. 1993; Baum and Wielicki 1994). The CO_2-slicing cloud heights have also been compared with those computed from lidar data (Smith and Platt 1978; Wylie and Menzel 1989; Smith and Frey 1990; Frey et al. 1999). Results show that the CO_2-slicing heights from low-spectral-resolution IR measurements (like those obtained from the High Resolution Infrared Radiation Sounder (HIRS; Smith et al. 1979), the GOES sounder, and the Moderate Resolution Imaging Spectroradiometer (MODIS) are within 50-hPa rmse of lidar, stereo, and other measurements. However, because of the limited number of comparisons taken over a small geographical area, the validation for the CO_2-slicing cloud-top heights is incomplete.

The Atmospheric Infrared Sounder (AIRS; details available online at http://www-airs.jpl.nasa.gov; Aumann et al. 2003) on NASA's Earth Observing System (EOS) *Aqua* satellite is a high-spectral-resolution ($\nu/\Delta\nu = 1200$) IR sounder with 2378 channels. AIRS radiances in the IR wavelength region of 3.74–15.4 μm enable the derivative of the vertical profiles of atmospheric temperature and water from the earth's surface to an altitude of 40 km with a horizontal resolution of 13.5 km at nadir. Taking advantage of high-spectral-resolution AIRS longwave cloudy radiance measurements, CTP and ECA can be retrieved with better accuracy than with MODIS. An approach called the minimum local emissivity variance (MLEV; Huang et al. 2004) technique has been tested for retrieving the CTP and ECA from high-spectral-resolution sounder radiances; the MLEV technique seeks the CTP solution with the minimum local cloud emissivity variance. However, the MLEV technique is not appropriate for operational processing because of its considerable computational requirements; overcast radiance calculations are needed from upper- to lower-level clouds for each longwave channel in order to seek the minimum. The CO_2-slicing algorithm can also be applied to retrieve CTP and ECA from AIRS radiances; however, it is difficult to select pairs from high-spectral-resolution sounder channels and give proper weight to each pair (Antonelli 2001; Smith and Frey 1990). In this paper, the one-dimensional variational method (1DVAR), using an iterative approach to find the solution, is shown to provide an efficient way to retrieve clouds using high-spectral-resolution sounder longwave cloudy radiance measurements. Since an AIRS-independent background is needed in the 1DVAR approach, the existing 5-km operational MODIS cloud product is an obvious choice. It should be noted that the current operational CTP products are created together with temperature and moisture sounding profiles using a cloud-clearing algorithm from combined AIRS and AMSU measurements (Susskind et al. 2003). The 1DVAR algorithm is a practical way for retrieving cloud parameters from imager and sounder systems without microwave data. In addition, this study using MODIS–AIRS data is also relevant to the utilization of data from Advanced Baseline Imager (ABI) and Hyperspectral Environmental Suite (HES) systems on GOES-R.

MODIS (details available online at http://modis.gsfc.nasa.gov/about/specs.html) is a key instrument of the EOS *Terra* and *Aqua* satellites for conducting global change research. It provides global observations of earth's land, oceans, and atmosphere in 36 visible (VIS), near infrared (NIR), and infrared (IR) regions of the spectrum from 0.4 to 14.5 μm. MODIS cloud products (details available online at http://modis.gsfc.nasa.gov/data/dataproducts.html) include, but are not limited to, the cloud mask (Ackerman et al. 1998), which provides each MODIS 1-km pixel with a clear index (confident clear, probably clear, confident cloudy, and probably cloudy); cloud phase, which provides each MODIS 1-km pixel with a phase index (water clouds, ice clouds, mixed phase, etc.); and CTP and ECA from MODIS CO_2 band measurements with a 5-km spatial resolution (King et al. 2003; Platnick et al. 2003).

The 1DVAR algorithm simultaneously accounts for the instrument noise, uncertainties in the radiative transfer model, atmospheric temperature and moisture effects, and the satellite measurements of clouds. Since all longwave CO_2 spectral cloudy radiances are 1) inversely weighted by their instrument noise plus the assumed forward model error and 2) used simultaneously in the 1DVAR retrieval processing, noticeable improvements in 1DVAR cloud retrievals were found over the CO_2-slicing cloud parameters (Li et al. 2001). A fast and accurate radiative transfer model called the Stand-Alone AIRS Radiative Transfer Algorithm (SARTA; Hannon et al. 1996; Strow et al. 2003; details available online at http://asl.umbc.edu/pub/rta/sarta/) was used for AIRS clear-sky atmospheric transmittance calculations; it has 100 pressure-layer (101 pressure levels) vertical coordinates from 0.005 to 1100 hPa. The calculations take into account the satellite zenith angle, absorption by well-mixed gases (including nitrogen, oxygen, etc.), water vapor (including the water vapor continuum), ozone, and carbon dioxide.

Synergistic use of high-spatial-resolution MODIS cloud products and high-spectral-resolution AIRS longwave cloudy radiance measurements, described in this paper, can be applied to process EOS direct broadcast MODIS–AIRS data. These techniques will be relevant to data from the Visible Infrared Imaging Radiometer Suite (VIIRS) and Cross-Track Infrared Sounder (CrIS)

on the National Polar-Orbiting Environmental Satellite System (NPOESS) and relevant to data from the Advanced Baseline Imager (Schmit et al. 2002) and Hyperspectral Environmental Suite system on GOES-R (Gurka and Schmit 2002).

Section 2 presents the formulation for calculating the AIRS longwave cloudy radiances and estimating the sensitivity of CTP and ECA to AIRS measurements. Section 3 describes the 1DVAR retrieval scheme, and section 4 presents some simulation results. Section 5 compares the operational MODIS and GOES sounder cloud products with the MODIS–AIRS 1DVAR cloud retrievals. The results and implications are discussed in section 6, and future extensions and conclusions are summarized in section 7.

2. Sensitivity of AIRS longwave radiances to cloud height and amount

For a given longwave AIRS channel at wavenumber ν, the measured clear-sky radiance is given by

$$R_{\rm clr} = \varepsilon_s B_s \tau_s - \int_0^{p_s} B\, d\tau(0, p) + (1 - \varepsilon_s) \int_0^{p_s} B\, d\tau^*, \quad (1)$$

where $R_{\rm clr}$ is the clear spectral radiance in the infrared region as seen by the satellite sensor; B is the Planck radiance, which is a function of $T(p)$; p is pressure; τ is the atmospheric transmittance function; subscript s denotes surface; $\tau^* = \tau_s^2/\tau$ is the downwelling transmittance function; and ε_s is the surface emissivity. The three terms on right side of Eq. (1) represent the surface radiation, atmospheric radiation, and surface-reflected downwelling atmospheric radiation, respectively, reaching the satellite sensor. For an overcast black ($\varepsilon_c = 1$) cloud at pressure p_c, the radiance ($R_{\rm cld}$) is given by

$$R_{\rm cld} = B_c \tau_c - \int_0^{p_c} B\, d\tau(0, p), \quad (2)$$

where subscript c denotes the cloud top. The upwelling radiance (R) for a partially cloud-filled footprint is given by

$$R = (1 - N\varepsilon_c) R_{\rm clr} + N\varepsilon_c R_{\rm cld}. \quad (3)$$

In this equation, the cloud emissivity ε_c is multiplied by the cloud fractional coverage N, and the quantity $N\varepsilon_c$ is referred to as the effective cloud amount. Scattering by the atmosphere is assumed to be negligible in all of the above.

Knowledge of the instrument performance and atmospheric transmittance function characteristics is necessary for estimating the accuracy of the cloud property retrievals. A linearized differential form of Eq. (3) with respect to the CTP and the ECA (Li et al. 2001),

$$\delta R = (R_{\rm cld} - R_{\rm clr}) \delta(N\varepsilon_c) + (N\varepsilon_c)\tau_c \frac{\partial B_c}{\partial p} \delta p_c, \quad (4)$$

yields the sensitivity functions $\partial R/\partial(N\varepsilon_c) = R_{\rm cld} - R_{\rm clr}$ and $\partial R/\partial p_c = (N\varepsilon_c)\tau_c(\partial B_c/\partial p)$ of the ECA and the CTP, respectively. The magnitude for ECA sensitivity is the radiance change (delta R) resulting from a change in ECA of 0.1, while the magnitude for CTP sensitivity is the radiance change resulting from a change in CTP of 10 hPa. Figure 1 shows the CTP sensitivity functions for an opaque ($N\varepsilon_c = 1$) cloud (right) and the ECA sensitivity functions (left) of AIRS longwave channels with wavenumbers ranging from 680 to 815 cm^{-1} for a subartic winter atmosphere (Fig. 1a) and a tropical atmosphere (Fig. 1b). The surface skin temperature is set to be equal to the surface air temperature in the sensitivity calculations. The ordinate is the vertical pressure from 100 to 1100 hPa with step sizes from 5 to 20 hPa, and the abscissa is the wavenumber for AIRS longwave channels with a step size of $\Delta\nu$ for wavenumber ν given by $\nu/\Delta\nu = 1200$. The red color indicates strong sensitivity, while the blue color presents weak sensitivity. Note that the actual sensitivity to CTP should be the magnitude in this figure times the ECA; therefore, thick clouds have more sensitivity to CTP than thin clouds. In general, mid- and high-level clouds (clouds above the 700-hPa level) have more sensitivity to ECA where the difference between clear and overcast radiances is large.

There are good CTP sensitivities for most cloud levels except very high and very low level clouds. The tropical atmosphere provides much better CTP information in the AIRS radiances for high- and low-level clouds (within 100 hPa) than a subarctic winter atmosphere (within 200 hPa). All AIRS longwave channels have maximum CTP sensitivities at approximately 400–600 hPa, which means clouds with a CTP inside this range are easier to retrieve than those with a CTP outside this range.

3. The 1DVAR retrieval scheme

The 1DVAR algorithm for AIRS CTP and ECA retrievals uses the operational MODIS CTP and ECA derived from the CO_2-slicing algorithm (Frey et al. 1999; Platnick et al. 2003) as background and first-guess information to calculate the nonlinear optimal solution of cloud parameters from the AIRS longwave spectral band cloudy radiance measurements. AIRS channels with wavenumbers between 650 and 790 cm^{-1} are used in the CTP and ECA retrieval. Given an AIRS-observed cloudy radiance, R, for each channel, then $R = R(T, q, T_s, \varepsilon_s, p_c, N\varepsilon_c)$ [see Eq. (3)], which has the form

$$\mathbf{Y} = F(\mathbf{X}), \quad (5)$$

where the vector $\mathbf{X}$ contains CTP and ECA [the atmospheric temperature profile $T(p)$, moisture profile $q(p)$, surface skin temperature T_s, and infrared surface

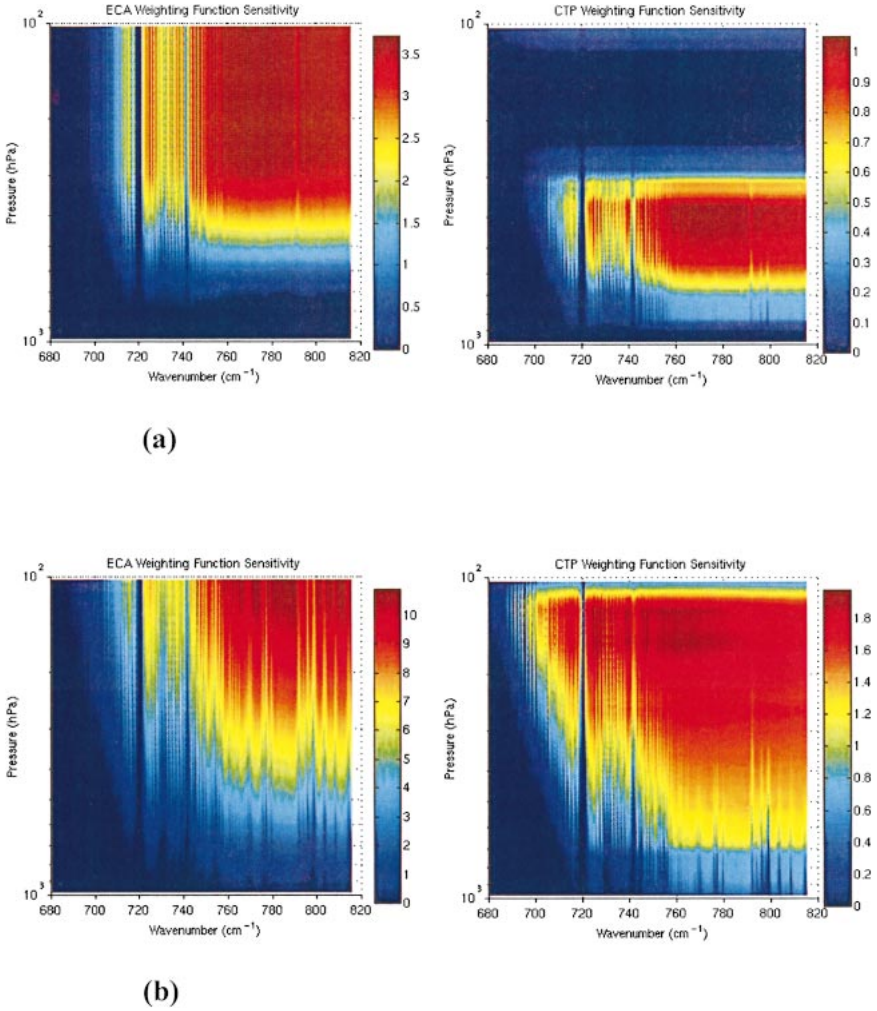

FIG. 1. The CTP sensitivity functions for (right) an opaque cloud and (left) the ECA sensitivity functions of AIRS longwave channels with wavenumbers ranging from 680 to 815 cm^{-1} with (a) a subarctic winter atmosphere and (b) a tropical atmosphere.

emissivity ε_s are assumed to be known or obtained from the European Centre for Medium-Range Weather Forecasts (ECMWF) forecast model analysis], and $\mathbf{Y}$ contains N satellite-observed cloudy radiances. The linear form of Eq. (5) is

$$\delta\mathbf{Y} = \mathbf{F}'\delta\mathbf{X}, \tag{6}$$

where $\mathbf{F}'$ is the linear or tangent model of the forward model $\mathbf{F}$, which is outlined by Eq. (4).

The 1DVAR approach is to minimize a penalty function $J(\mathbf{X})$, which measures how well the radiance measurements fit the background information and possibly other physical constraints. A general form of the 1DVAR solution (Rodgers 1976; Eyre 1989) is given by

$$J(\mathbf{X}) = [\mathbf{Y}^m - \mathbf{Y}(\mathbf{X})]^{\mathrm{T}}\mathbf{E}^{-1}[\mathbf{Y}^m - \mathbf{Y}(\mathbf{X})] + (\mathbf{X} - \mathbf{X}_B)^{\mathrm{T}}\mathbf{B}^{-1}(\mathbf{X} - \mathbf{X}_B), \tag{7}$$

where the vector $\mathbf{X}$ contains the CTP and ECA that need to be solved. Since ECA is spectrally dependent, ECAs at 10 wavenumbers (710, 720, 730, 740, 750, 760, 770, 780, 790, and 800 cm^{-1}) are retrieved, and ECA for a given channel will be obtained by linear interpolation from these 10 ECAs. Here, $\mathbf{X}_B$ is the background information inferred from the MODIS operational CTP and ECA products; $\mathbf{Y}^m$ is the vector of the AIRS-measured cloudy radiances used in the retrieval process; $\mathbf{Y}(\mathbf{X})$ is a vector of cloudy radiances calculated from the cloud state $\mathbf{X}$; $\mathbf{E}$ is the observational error covariance matrix, which includes instrument noise plus the assumed forward model error; and $\mathbf{B}$ is the assumed background error covariance matrix, which constrains the solution. To solve Eq. (7), a Newtonian iteration is used:

$$\mathbf{X}_{n+1} = \mathbf{X}_n + J''(\mathbf{X}_n)^{-1}J'(\mathbf{X}_n), \tag{8}$$

where J' is the first derivative of the cost function, and J'' is the second derivative. The following quasi-nonlinear iterative form (Eyre 1989) is obtained:

$$\delta\mathbf{X}_{n+1} = (\mathbf{F}_n^{\mathrm{T}}\mathbf{E}^{-1}\mathbf{F}_n' + \mathbf{B}^{-1})^{-1}\mathbf{F}_n^{\mathrm{T}}\mathbf{E}^{-1}(\delta\mathbf{Y}_n + \mathbf{F}_n'\delta\mathbf{X}_n), \quad (9)$$

where $\delta\mathbf{X}_n = \mathbf{X}_n - \mathbf{X}_B$, $\delta\mathbf{Y}_n = \mathbf{Y}^m - \mathbf{Y}(\mathbf{X}_n)$, and $\mathbf{F}_n'$ from Eq. (6) represents the linear terms with δR expansion of Eq. (4).

The background error covariance matrix $\mathbf{B}$ is assumed to be diagonal with a standard deviation (square root of the diagonal element) of 50 hPa for the MODIS CTP error and 0.15 for the MODIS ECA. The logarithm of CTP is used to stabilize the solution of Eq. (9), and the background error for $\ln p_c$ is $\Delta \ln p_c = \Delta p_c/p_c \sim 0.01$, assuming that the averaged CTP is 500 hPa. The measurement error covariance matrix $\mathbf{E}$ is a fixed diagonal matrix, where each diagonal element is the square of the AIRS instrument noise plus an assumed forward model error of 0.2 K for each longwave channel. The first guess $\mathbf{X}_0$, or the starting point of the iteration in Eq. (9), is also from the MODIS CTP and ECA product.

4. A simulation of AIRS–MODIS cloud retrievals

To evaluate the MODIS–AIRS (1DVAR retrieval from AIRS radiances with the MODIS product as the background and first-guess information) improvement over either the MODIS-alone or AIRS-alone cloud parameters, a simulation study was conducted initially. The AIRS-alone 1DVAR takes an estimate of CTP and ECA from the minimum residual (MR) method as the background and first-guess information. The MR method seeks the CTP and a wavenumber-independent ECA by minimizing the differences between observations and calculations using CO_2 channels between 750 and 790 cm^{-1}. Therefore, the estimate of the cloud-top pressure p_c^0 and effective cloud amount $N\varepsilon_c^0$ is given by

$$\delta^2(p_c^0, N\varepsilon_c^0) = \min\delta^2(p_c, N\varepsilon_c), \quad (10)$$

where

$$\delta^2(p_c, N\varepsilon_c) = \sum_j [R_j^m - R_j(p_c, N\varepsilon_c)]^2, \quad (11)$$

R is calculated by Eq. (3), and the summation is over channels between 750 and 790 cm^{-1}. See Eyre and Menzel (1989) for details on MR. It should be noted that the MR procedure is time consuming since more overcast radiance calculations are needed from upper- to low-level clouds for each AIRS channel in order to seek the minimum. This procedure can also be applied to MODIS-alone 1DVAR retrievals.

For this simulation, 450 global radiosonde profiles representing various atmospheric conditions were selected, and 40 combinations were formed from each profile by assigning four CTPs (200, 300, 550, and 850 hPa plus a 50-hPa random variation corresponding to very high, high-, mid-, and low-level clouds) and 10 ECAs (0.1, 0.2, 0.3, 0.4, 0.5, 0.6, 0.7, 0.8, 0.9, and 1.0). The MODIS and AIRS longwave cloudy radiances were simulated [using Eqs. (1)–(3)] for all combinations of each profile. A spectrally constant ECA for both MODIS and AIRS was assumed in the simulated MODIS and AIRS cloudy radiances, while an infrared surface emissivity of 0.98 for each AIRS longwave channel and MODIS spectral band was assumed in the simulated radiance. The AIRS instrument noise (see Fig. 16 for the AIRS instrument noise of granule 193 on 06 September 2002) plus a forward model error of 0.2 K were randomly added to each AIRS channel cloudy radiance calculation. Also the MODIS instrument noise plus a forward model error of 0.2 K were added to each MODIS spectral band. The radiative transfer calculation of the MODIS spectral radiances is performed using a transmittance model called the Pressure-Layer Fast Algorithm for Atmospheric Transmittances (PFAAST; Hannon et al. 1996); this model also has 101 pressure-level vertical coordinates from 0.05 to 1100 hPa. The calculations take into account the satellite zenith angle and absorption by well-mixed gases (including nitrogen, oxygen, and carbon dioxide), water vapor (including the water vapor continuum), and ozone. The simulation study focused on the following three configurations:

1) MODIS-alone 1DVAR, where the CTP and ECA estimates from MODIS radiances using the MR method serve as the background and first-guess information—1DVAR was performed with MODIS radiances.
2) AIRS-alone 1DVAR, where CTP and ECA estimates from AIRS radiances between 750 and 790 cm^{-1} using the MR method serve as the background and first-guess information—1DVAR was performed with AIRS radiances between 650 and 790 cm^{-1}.
3) MODIS–AIRS 1DVAR, where CTP and ECA estimates from MODIS radiances using the MR method serve as the background and first-guess information—1DVAR was performed to the AIRS radiances between 650 and 790 cm^{-1}.

For atmospheric temperature, a 1.5-K random error was assumed at each pressure level, which is close to the accuracy of the forecast model analysis. A 15% error was included for the water vapor mixing ratio at each pressure level. For surface skin temperature a random error of 2.5 K was assumed and a 1.5% error was included for IR surface emissivity. Figure 2 shows the retrieved CTP root-mean-square error (rmse) with respect to truth for the MODIS-alone 1DVAR, AIRS-alone 1DVAR, and MODIS–AIRS 1DVAR retrievals for the four cloud types. MODIS–AIRS 1DVAR significantly reduces the MODIS-alone 1DVAR CTP rmse by 10–40 hPa for most clouds. AIRS-alone 1DVAR is much better than MODIS-alone 1DVAR because of the high spectral resolution of AIRS radiances. Overall, MODIS–AIRS 1DVAR is slightly better than AIRS-alone 1DVAR, but MODIS–AIRS 1DVAR is slightly worse than AIRS-alone 1DVAR for very thin high cloud because of the poor first guess from MODIS for very thin clouds. The AIRS-alone 1DVAR changes the AIRS MR results slightly, as does the MODIS-alone 1DVAR

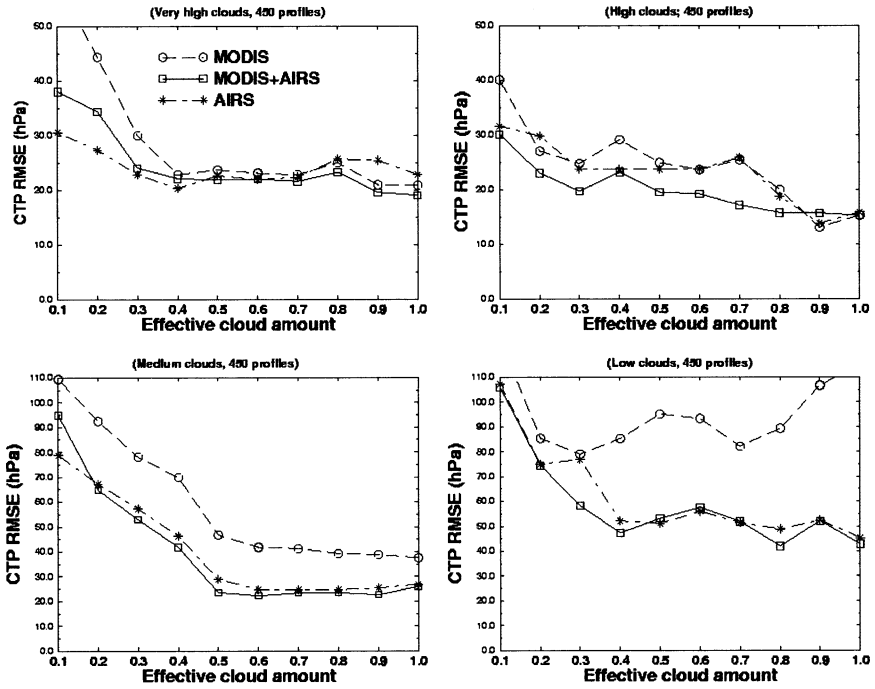

FIG. 2. The retrieved CTP rmse with respect to truth for the MODIS-alone 1DVAR, AIRS-alone 1DVAR, and MODIS–AIRS 1DVAR retrievals for the four cloud types (very high, high-, mid-, and low-level clouds).

(not shown), because of the fact that most CO_2 channel radiances are already used in the MR method. However, 1DVAR is able to retrieve the spectrally dependent ECA, while the MR only gives a spectrally independent ECA.

5. Retrieval of cloud parameters from AIRS longwave radiance measurements

The operational MODIS cloud products using the CO_2-slicing technique are used as the background information and first guess in the MODIS–AIRS 1DVAR processing with AIRS radiance measurements, and the results from MODIS–AIRS are compared with MODIS operational products in the following discussion. A granule of AIRS data was studied. Each granule contains 135 lines with each line containing 90 pixels. Figure 3 shows the AIRS longwave window channel 763 (901.69 cm^{-1}) brightness temperature (BT) images at 1917 UTC 6 September 2002. The red color indicates warm scene or clear skies, while the blue color represents a cold scene or cloudy skies. Collocated MODIS data were used for the AIRS CTP and ECA retrieval study. The 1-km MODIS pixels are collocated to each AIRS footprint. The collocation accuracy is better than 1 km provided that the geometry information from both instruments is accurate (Li et al. 2004). Radiances from 14 MODIS spectral bands are used to estimate whether a given view of the earth's surface is affected by clouds, aerosol, or shadow (Ackerman et al. 1998), and the resulting MODIS operational cloud mask, MYD35, is used in this study. The AIRS footprint is determined to be cloudy for cloud retrieval only when the percentage of the clear MODIS pixels within the AIRS footprint is less than 10%. The atmospheric temperature and moisture profiles as well as the surface skin temperature are taken from the ECMWF forecast model analysis in the 1DVAR retrieval. The iteration,

$$\chi_i = |\mathbf{X}_i - \mathbf{X}_{i-1}|, \tag{12}$$

is monitored for divergence (when $\chi_{i+1} > \chi_i$, within two iterations, the iteration is stopped, and the retrieval is assumed to have failed) and convergence (when $\chi < 0.5$ or a maximum of six iterations is reached). In each iteration, the CTP is limited to 115 hPa for the highest and 1000 hPa for the lowest, while the ECA must be between 1.0 and 0. Only AIRS longwave channels with observed-minus-calculated BTs greater than 3 times the instrument noise are used in the 1DVAR; 1DVAR will not be attempted if less than five AIRS channels are found.

The 1-km MODIS CTPs and ECAs (expanded from operational 5-km products) within each AIRS footprint are averaged as

$$\overline{p}_c = \frac{\sum_j p_c^j (N\varepsilon_c^j)}{\sum_j (N\varepsilon_c^j)} \quad \text{and} \tag{13a}$$

$$\overline{N\varepsilon}_c = \frac{1}{J}\sum_j (N\varepsilon_c^j), \tag{13b}$$

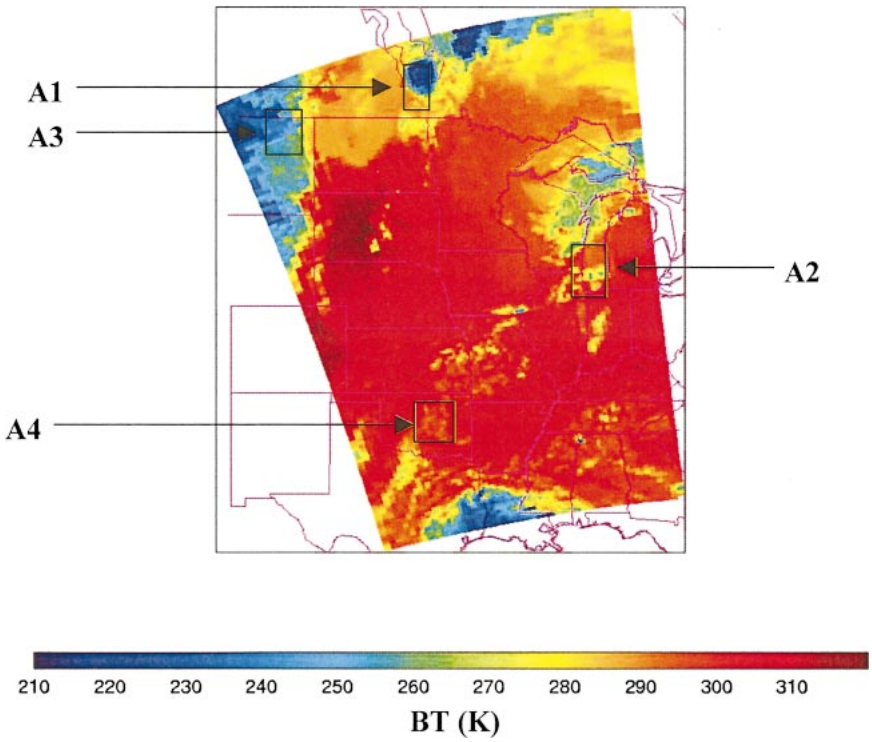

FIG. 3. The AIRS longwave window channel 763 (901.69 cm^{-1}) BT image at 1917 UTC 6 Sep 2002 (AIRS granule 193).

where $j(j = 1, 2, \ldots, J)$ is the index of the MODIS 1-km pixels within the AIRS footprint, J is the total number of MODIS 1-km pixels collocated to the AIRS footprint, and $\overline{p}_c$ and $\overline{N\varepsilon}_c$ are used as the background and the first-guess information for the 1DVAR cloud retrieval for that AIRS footprint.

In the selected granule, 6332 AIRS footprints were detected to be cloudy, and 5232 had successful cloud retrievals (83%). For the remaining 1100, the residual between measured and calculated (from the MODIS CTP and ECA background information) brightness temperatures was too small (8%) or the cloud retrieval failed to converge (9%); nonconvergence occurred primarily in multilayer cloud conditions as estimated by the MODIS classification (Li et al. 2003).

Several AIRS footprints are selected for detailed analysis. These footprints include two that have thick high-level and thick low-level clouds, two that have partial clouds, and one that has midlevel clouds. Figure 4 shows the study area A1 (see Fig. 3 for the location) with the MODIS classification mask collocated to the AIRS footprints. Single-layer high clouds or low clouds within the AIRS footprints are well identified by the MODIS classification mask. Some AIRS footprints contain multilayer clouds (e.g., mixed mid- and low-level clouds). Footprints F1 (line 125, pixel 44) and F2 (line 121, pixel 41) represent thick high clouds and low clouds, respectively, according to the MODIS classification mask. Footprint F1 is determined to be ice clouds while F2 is water clouds based on the MODIS cloud phase mask. Figure 5 (top) shows the AIRS longwave cloudy BT calculation [see Eq. (3)] from the MODIS CTP and ECA (dotted line), the BT calculation from the MODIS–AIRS-retrieved CTP and ECA [see Eq. (9); long dashed line], and the cloudy BT observation (solid line) spectra for footprint F1. Figure 5 (bottom) shows the corresponding BT difference between observation and calculation. Figure 6 is the same as Fig. 5, but for footprint F2. In general, MODIS did very well for thick clouds—there is only a slight change in the MODIS–AIRS CTP from the MODIS CTP; however, there is a better fit between the calculation and observation with the MODIS–AIRS CTP and ECA than with the MODIS cloud products.

Figure 7 shows the study area A2 (Lake Michigan area; see Fig. 3). Footprints F3 (line 70, pixel 80) and F4 (line 69, pixel 79) view ice clouds in partly cloudy conditions. Figure 8 shows that MODIS–AIRS produces only slight changes in the MODIS CTP in this very thin cloud in footprint F3; however, MODIS–AIRS changes the MODIS ECA by 0.05, which results in a significant BT difference, according to Fig. 1. Although the calculation with MODIS–AIRS-retrieved CTP and ECA fits the observation very well in the CO_2 region (650–790 cm^{-1} or 12.66–15.38 μm), there is still a discrepancy between the calculation and observation in the IR window region (900–1130 cm^{-1} or 8.85–11.11 μm) due to the scattering in ice clouds.

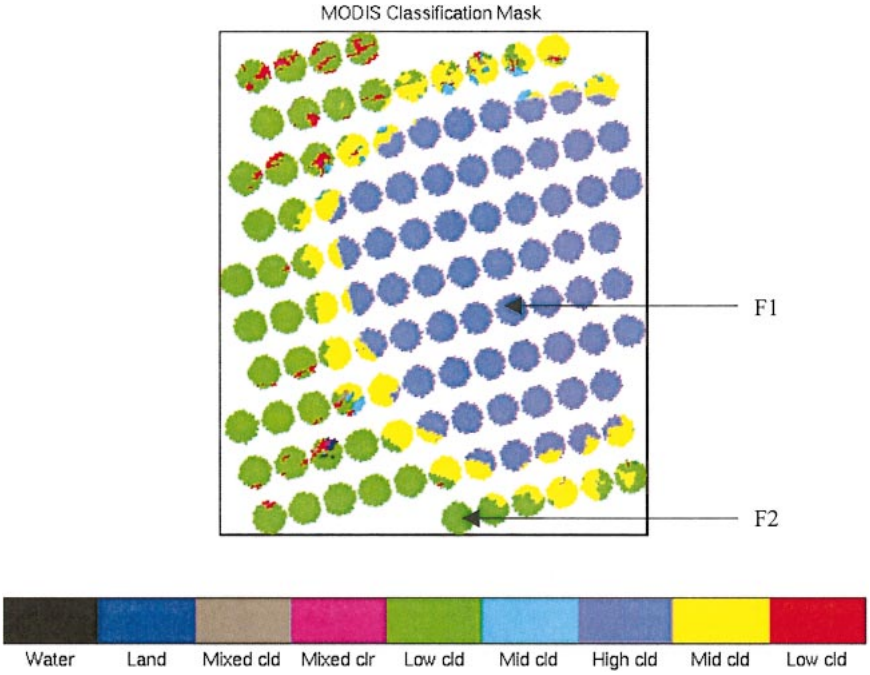

FIG. 4. The study area A1 (see Fig. 3) of MODIS classification mask collocated to AIRS footprints. Footprints F1 and F2 are classified as thick high clouds and low clouds, respectively.

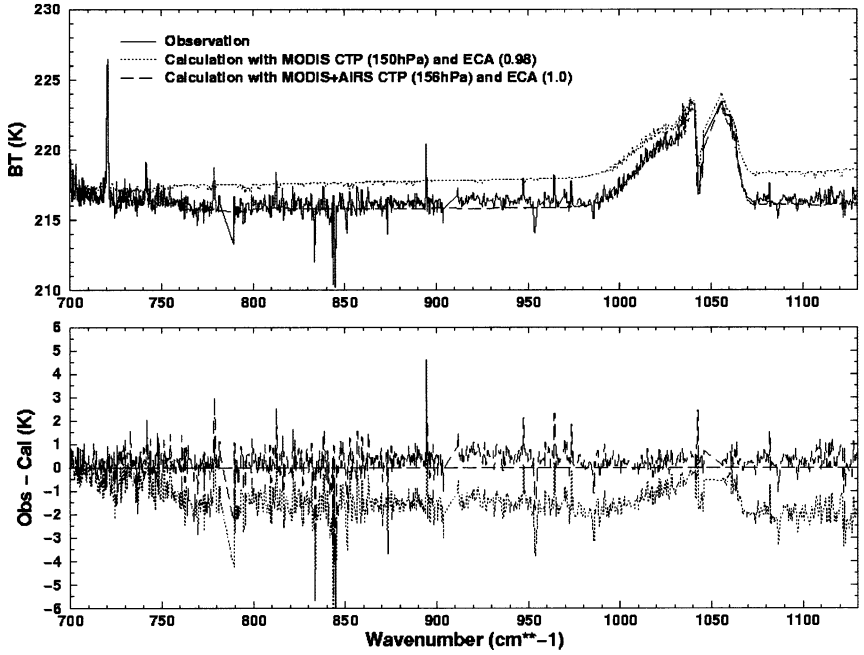

FIG. 5. (top) The AIRS longwave cloudy BT calculation with the operational MODIS CTP and ECA (dotted line), the BT calculation with the MODIS–AIRS-retrieved CTP and ECA (long dashed line), and the cloudy BT observation (solid line) spectra for footprint F1. (bottom) The corresponding BT difference between the observation and the calculation (obs − calc).

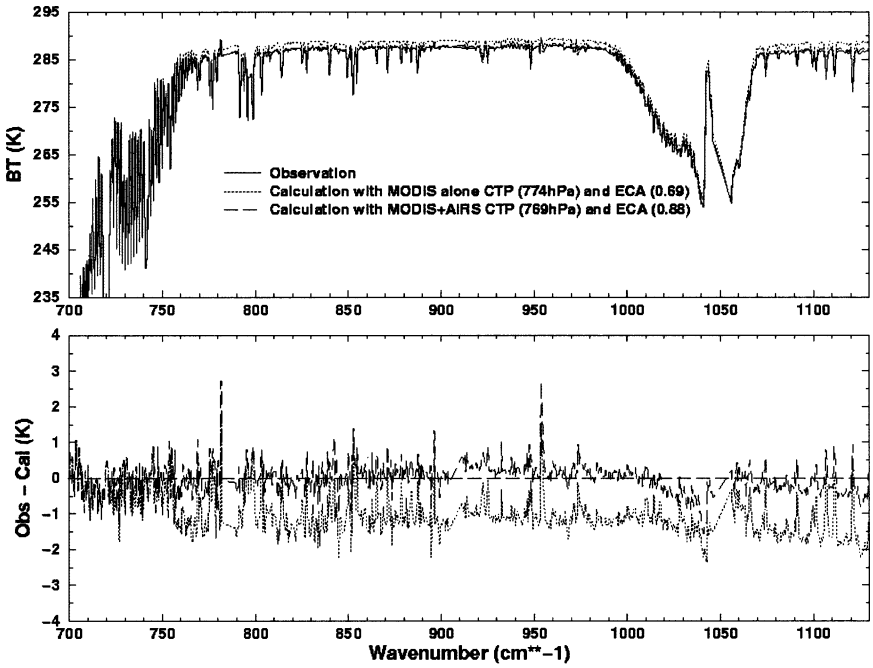

FIG. 6. Same as in Fig. 5, but for F2.

In order to account for the scattering and absorption effects in ice clouds and water clouds, a fast radiative transfer cloudy model for a hyperspectral IR sounder is being developed through joint efforts at the University of Wisconsin—Madison and the Texas A&M University. In the fast cloudy radiative transfer model, single scattering in ice clouds assumes hexagonal shapes for large particles and droxtals for small particles (Yang et al. 2001, 2003). For water clouds, spherical water droplets are assumed. The Lorenz–Mie theory is used to calculate the single-scattering properties. The cloud microphysical properties are described in terms of cloud

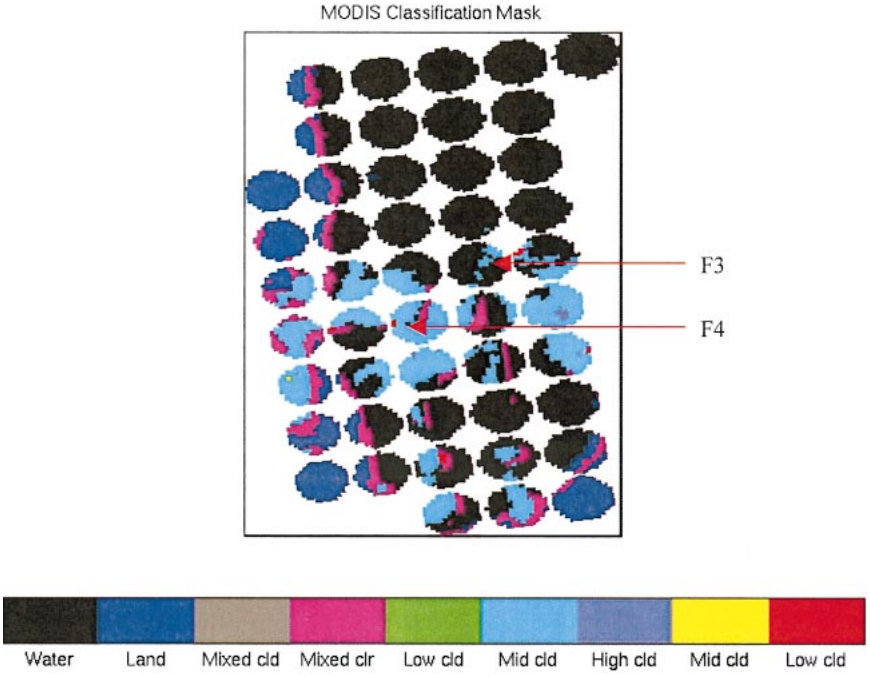

FIG. 7. The study area A2 (Lake Michigan area; see Fig. 3) of the MODIS classification mask collocated to the AIRS footprints.

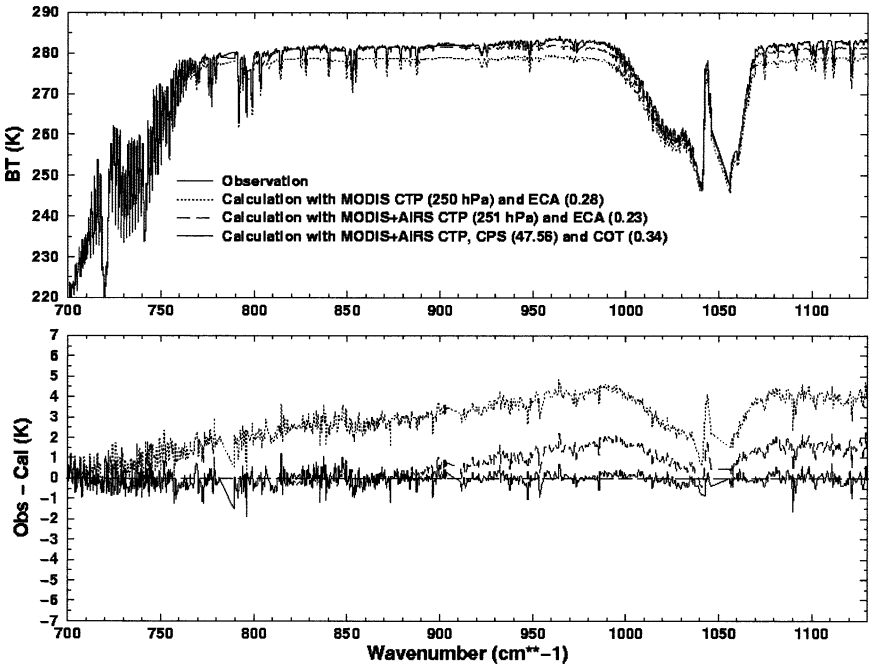

FIG. 8. Same as Fig. 5, but for F3.

particle size (CPS) in diameter and visible cloud optical thickness (COT). Given the visible COT and CPS, the IR COT, single-scattering albedo, and asymmetry factor can be parameterized for radiative effects of ice clouds and water clouds. The cloudy radiance for a given AIRS channel can be calculated by combining the clear-sky optical thickness from SARTA and the cloud effects by adding a COT, single-scattering albedo, and scattering phase function. Studies show that the slope of an IR cloudy BT spectrum between 790 (12.6 μm) and 960 cm^{-1} (10.4 μm) is sensitive to the CPS, while the cloudy radiances are sensitive to COT in the region from 1050 (9.5 μm) to 1250 cm^{-1} (8 μm) for ice clouds (Chung et al. 2000; Wei et al. 2004, hereinafter W04).

From the determined CTP, the CPS and COT can be retrieved simultaneously from 800 (12.5 μm) to 1130 cm^{-1} (8.8 μm), also using the variational approach. The MODIS CPS and COT products serve as the background and first-guess information as before. The details on the fast cloudy radiative transfer model and the retrieval of cloud microphysical properties (CPS and COT) are described in another paper (Li et al. 2004, manuscript submitted to *J. Appl. Meteor.*). Calculations (thick solid line) that include the MODIS–AIRS estimates of CPS and COT fit the observations (thin solid line) quite well for all AIRS longwave channels shown in Fig. 8 for footprint F3. Figure 9 is the same as Fig. 8, but for footprint F4, which has more ice cloud cover. The AIRS radiance measurements raise the MODIS CTP by 17 hPa, while they decrease the MODIS ECA by approximately 0.05; the calculation fits the observation better after this CTP and ECA adjustment from the AIRS radiance measurements. Again, there is a significant difference between the calculation and the observation in the window region [see Eq. (3)]; this discrepancy is almost removed by accounting for the effects of the cloud particle size. The BT calculation with CPS and COT fits the slope of the observation very well.

Figure 10 shows the study area A3 (see Fig. 3) of the MODIS classification mask collocated to the AIRS footprints. Footprint F5 (line 126, pixel 10) indicates midlevel ice clouds according to the MODIS classification mask and the MODIS cloud phase mask. Figure 11 shows that there is a large difference between calculation with the MODIS cloud products and observation in the CO_2 region. However, the difference in the CO_2 region is almost removed by the calculation with the AIRS-retrieved CTP and ECA; AIRS adjusted the MODIS CTP by 68 hPa. The slope of the BT in the spectral window region for F5 is significantly larger than that found in F3 and F4, suggesting smaller CPS. With AIRS-retrieved CPS and COT for this footprint, the calculation (thick solid line) fits the observation (thin solid line) slope very well, indicating that the cloud microphysical properties can be retrieved effectively by the AIRS radiance measurements. W04 have compared AIRS COT retrievals with MODIS COT products; the correlation is very high, but AIRS can also provide nighttime retrievals.

Figure 12 shows the 6 September 2002 operational MODIS 5-km CTP (upper left), the AIRS-alone 14-km CTP (upper right), the GOES sounder 10-km CTP (lower left), and MODIS–AIRS 14-km CTP (lower right) for 1917 UTC (the time for the GOES sounder retrievals

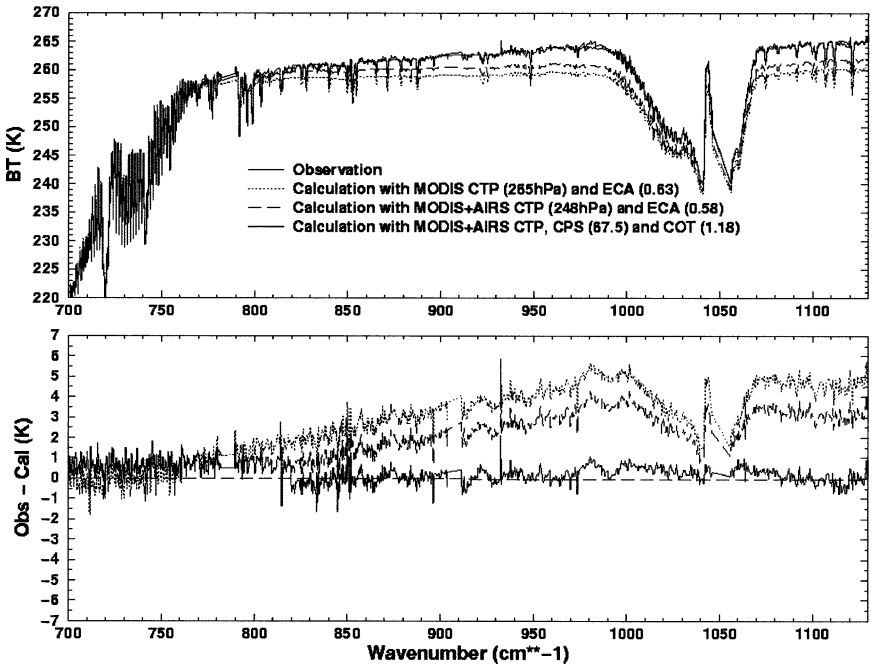

FIG. 9. Same as in Fig. 5, but for F4.

is 1846 UTC). The GOES sounder CTP retrieval (Schreiner et al. 2001) and the operational MODIS CTP use the National Centers for Environmental Prediction (NCEP) Global Data Analysis System (GDAS) analysis, while the AIRS-alone CTP and MODIS–AIRS retrievals use the ECMWF forecast model analysis. Different forecast analyses should not result in significantly different CTP retrievals, according to Menzel et al. (1992). Figure 13 shows the associated scatterplot between collocated MODIS–AIRS and the operational MODIS or the GOES sounder CTPs for AIRS single-layer clouds [single-layer clouds are determined by the MODIS classification

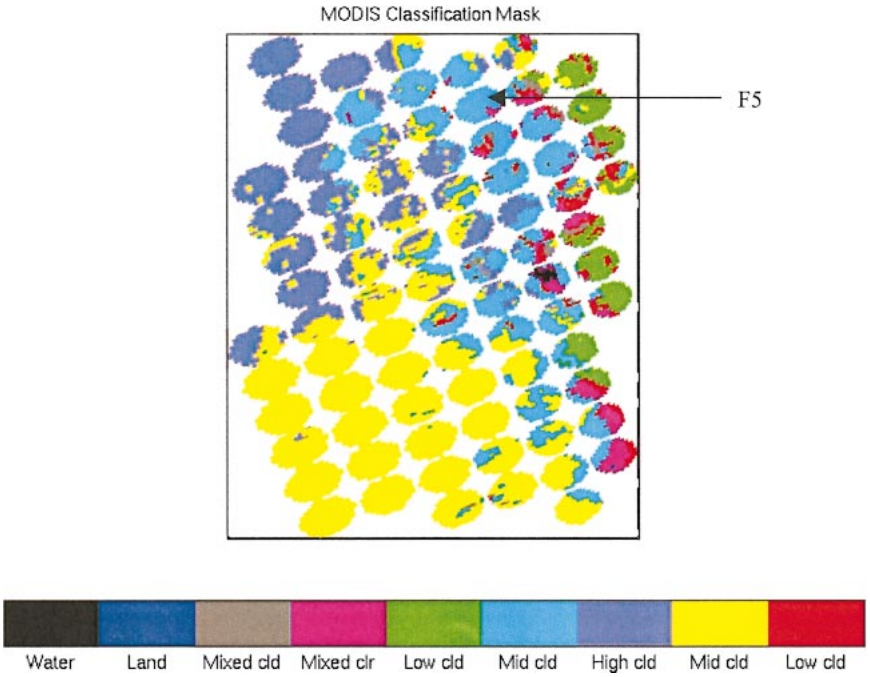

FIG. 10. The study area A3 (see Fig. 3) of the MODIS classification mask collocated to AIRS footprints.

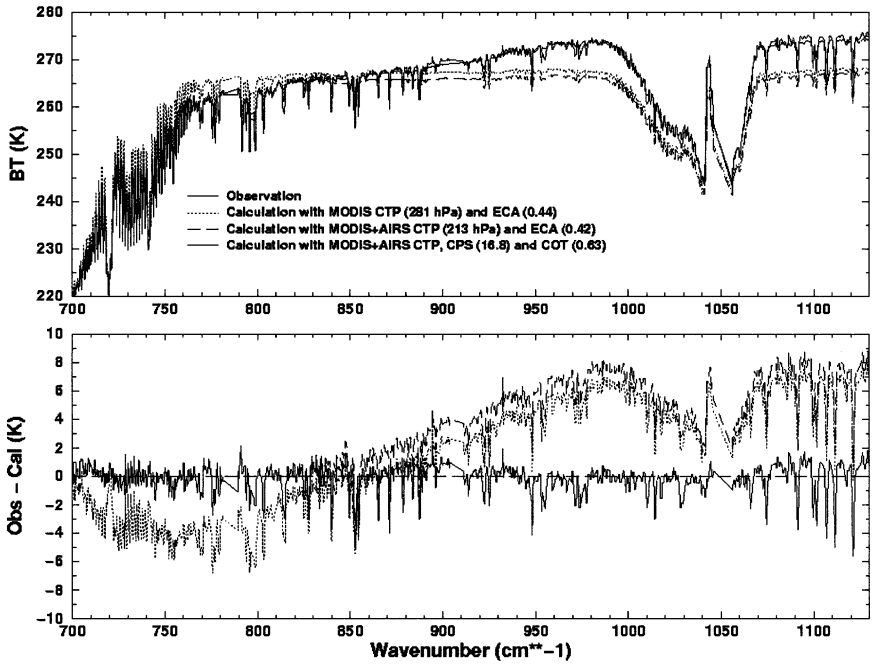

FIG. 11. Same as in Fig. 5, but for F5.

mask (Li et al. 2004)] from granule 193 on 6 September 2002. In general, both MODIS and GOES sounder CTPs agree well with MODIS–AIRS CTPs; the discrepancies between GOES sounder CTPs and the MODIS–AIRS CTPs might be due to the multilevel clouds within the GOES sounder field of view (FOV), although the AIRS footprint contains single-layer clouds. Spatial and temporal differences between AIRS and the GOES sounder also result in some CTP differences. Figure 14 is the same as Fig. 13, but for a scatterplot between MODIS–AIRS and the operational MODIS or the AIRS-alone CTPs. Both operational MODIS CTPs and AIRS-alone CTPs have a high correlation with MODIS–AIRS CTPs, but MODIS–AIRS CTPs should have better accuracy than the operational MODIS CTPs, according to the above study.

For validation, MODIS–AIRS cloud-top heights (CTHs) at the Atmospheric Radiation Measurement–Cloud and Radiation Test Bed (ARM–CART) site in Purcell, Oklahoma were compared with the ground-based Vaisala Ceilometer (VCEIL) (Lonnqvist 1995) cloud-base height (CBH) measurements. The CTH should be higher than the CBH if the retrieval is correct. The four nearest AIRS footprints (F6, F7, F8, and F9) surrounding the ARM–CART site at Purcell in the small area A4 (see Fig. 3) were selected for comparison. The MODIS true color image (not shown) indicates that thin and very low level clouds exist in this area; the MODIS classification mask also indicates very thin and low clouds within the four AIRS footprints. The CTHs retrieved by MODIS–AIRS and the operational MODIS CTHs for the four footprints are listed in Table 1. MODIS–AIRS and MODIS have similar CTHs for footprints F6 and F7; both are close to the VCEIL CBH. However, MODIS–AIRS significantly lowers the CTHs from the MODIS CTHs for F8 and F9, and the MODIS–AIRS CTHs are closer to the VCEIL CBHs than the MODIS CTHs for these two AIRS footprints.

6. Discussion

Synergistic use of MODIS cloud products and AIRS radiance measurements improves cloud property estimation. Using MODIS cloud products (CTP and ECA) as the background information and first guess in the AIRS variational retrieval and using the abundant spectral information of AIRS measurements to identify the cloud microphysical properties (CPS and COT), the MODIS–AIRS cloud parameter retrievals improve in comparison with other measurements. Instrument noise impacts the retrievals for some clouds (Li et al. 2001). After instrument noise, the largest source of error is the radiative transfer model uncertainty. Radiance biases can significantly influence the CTP and ECA retrievals; a bias adjustment is suggested to tune the radiance calculation (Seemann et al. 2003). Uncertainties in atmospheric temperature/moisture profiles, surface skin temperature from forecast model analysis, and surface emissivity estimation also influence the cloud property retrievals.

In order to study the AIRS cloud retrieval stability, the following three configurations are investigated using AIRS granule-193 data:

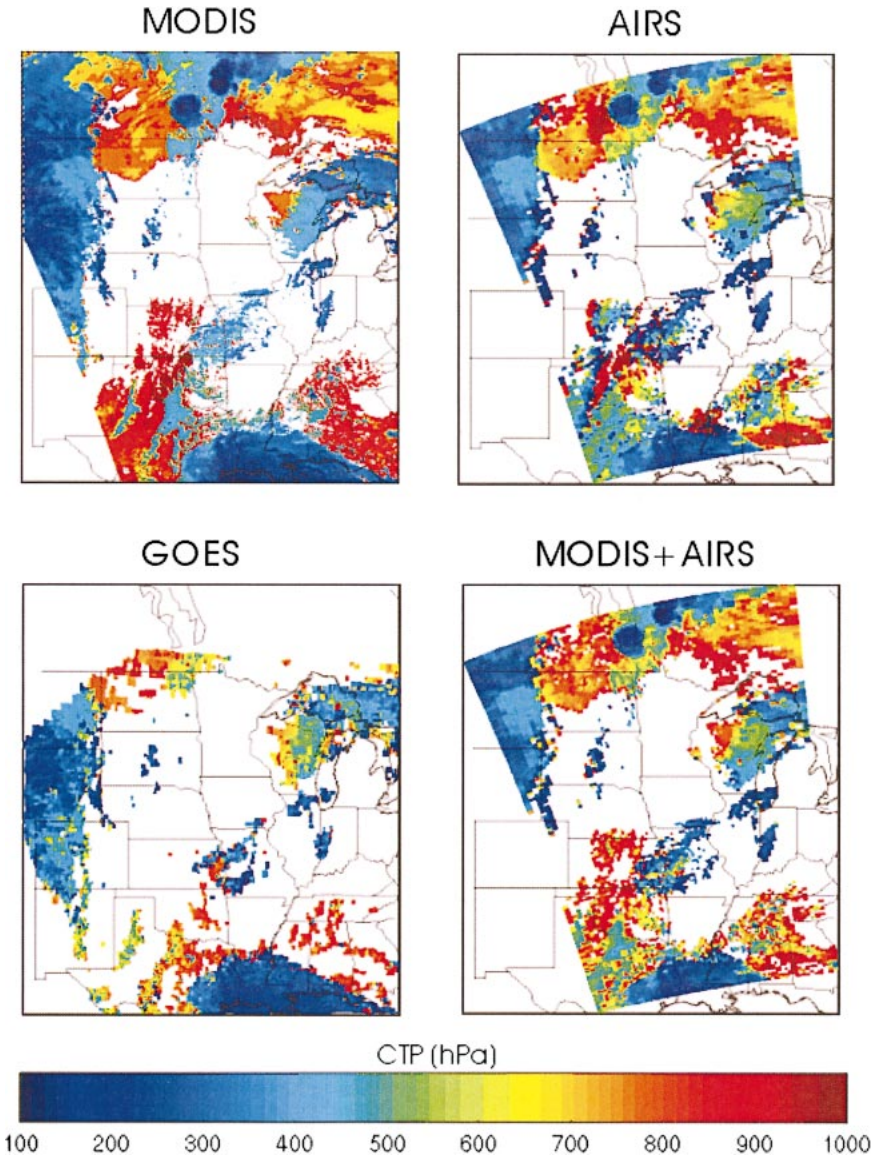

FIG. 12. (top left) The operational MODIS 5-km CTP, (top right) AIRS-alone 14-km CTP, (bottom left) the GOES sounder 10-km CTP, and (bottom right) MODIS–AIRS 14-km CTP for 1917 UTC (the time for the GOES sounder is 1846 UTC) 6 Sep 2002.

1) Background CTPs are increased by 50 hPa for all AIRS footprints.
2) Background CTPs are decreased by 50 hPa for all AIRS footprints.
3) Background CTPs with 50 hPa (standard deviation) are added.

Figure 15 shows the scatterplot between MODIS–AIRS CTPs versus MODIS–AIRS CTPs from the three configurations listed above; the MODIS–AIRS CTP retrievals appear to be stable with respect to the background information. Cloud retrievals in most footprints do not show a significant change after the background information is altered.

The BT residuals between calculation and observation, along with the root mean square of the noise equivalent temperature difference (rms NeDT) from all the AIRS cloudy footprints in the granule are shown in Fig. 16. The BT residual rms with the MODIS CTP and ECA products remains large in the CO_2 region, while they are reduced significantly by the MODIS–AIRS CTP and ECA retrievals. The BT residual rms with AIRS CTP and ECA retrievals is less than 1 K for most CO_2 channels although it is larger than the NeDT; it remains large in the window region (not shown) because of scattering or absorption. Figure 9 suggests that the window region differences are removed by introducing AIRS estimates of CPS and COT in the calculation of radiances. Li et al. (2004, manuscript submitted to *J. Appl. Meteor.*) contains more details.

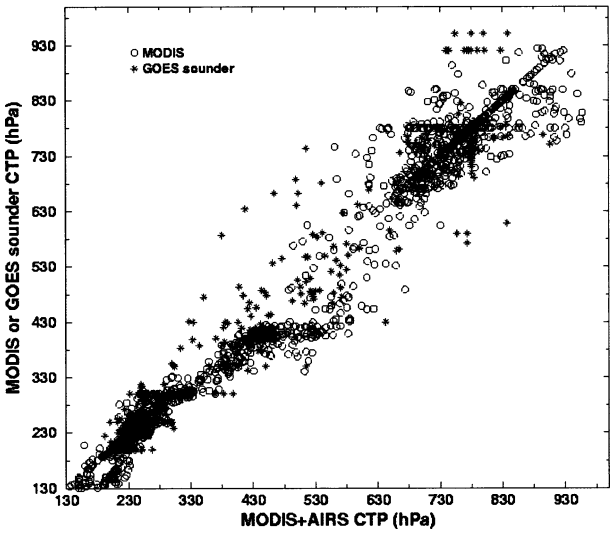

FIG. 13. The scatterplot between collocated MODIS–AIRS CTPs and the operational MODIS CTPs (circles) or the GOES sounder CTPs (stars) for the AIRS single-layer clouds of granule 193 on 6 Sep 2002.

7. Conclusions

An approach for the synergistic use of MODIS cloud product estimates and AIRS radiance measurements to retrieve cloud height and amount is described in this paper. CTP and ECA derived from the MODIS operational algorithm are used as background and first-guess information in the AIRS 1DVAR retrieval processing. Results suggest that the AIRS–MODIS retrievals compare better with other cloud measurements (radiosonde and ceilometer). In addition, spectra calculations using MODIS–AIRS cloud properties agree quite well with actual AIRS measurements.

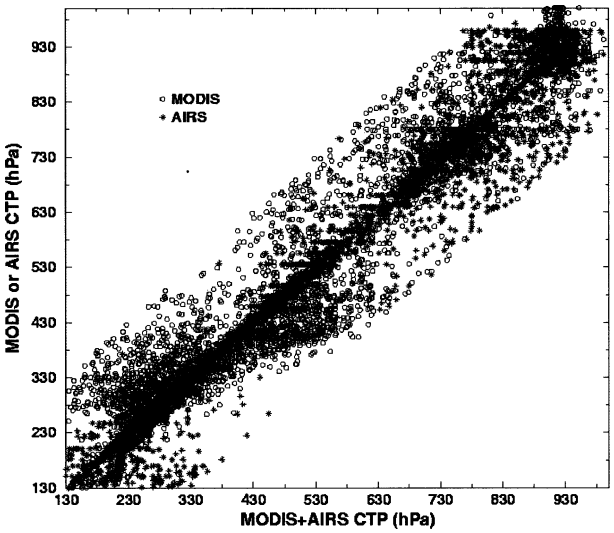

FIG. 14. The scatterplot between collocated MODIS–AIRS CTPs and the operational MODIS CTPs (circles) or the AIRS-alone CTPs (stars) for the AIRS granule 193 on 6 Sep 2002.

TABLE 1. The cloud-top heights retrieved by AIRS and MODIS measurements for the four nearest AIRS footprints surrounding the ARM–CART site at Purcell, OK.

Instruments	F6	F7	F8	F9
MODIS CTH (km)	1.475	1.475	2.760	2.510
MODIS–AIRS CTH (km)	1.468	1.452	1.730	1.483
VCEIL CBH (km)	1.100	1.100	1.100	1.100
MODIS–AIRS COT	0.278	0.185	0.070	0.065

Specifically, the following can be concluded:

1) Improvement of 10–40 hPa in rmse was found for the MODIS–AIRS 1DVAR over the MODIS cloud product retrievals in a simulation study.
2) MODIS–AIRS 1DVAR improves the AIRS-alone 1DVAR slightly and is much more efficient in terms of computation.
3) MODIS–AIRS CTPs and the GOES sounder CTPs show similar overall cloud patterns.
4) Forward calculations using MODIS–AIRS 1DVAR retrieved CTP and ECA fit the AIRS observations very well in the CO_2 region; however, scattering and absorption effects have to be accounted for in the calculations to fit the AIRS observation in the longwave window region.
5) Validation efforts in a small number of comparisons over the ARM–CART site show that MODIS–AIRS improves MODIS cloud property retrievals in low and thin clouds.
6) Sensitivity studies show that changing the background information has a moderate effect on the MODIS–AIRS 1DVAR retrieval, implying that the MODIS–AIRS cloud retrieval is stable in most situations.

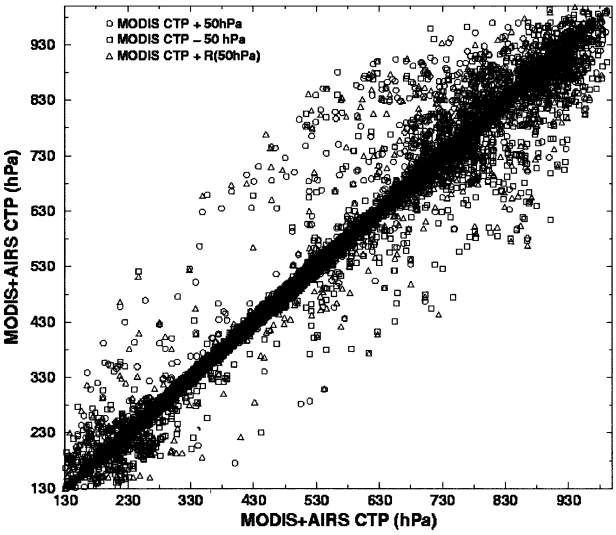

FIG. 15. The scatterplot between MODIS–AIRS CTPs vs MODIS–AIRS CTPs from the three configurations: MODIS CTP + 50 hPa (circles), MODIS CTP − 50 hPa (squares), and MODIS CTP + R (50 hPa; triangles), respectively.

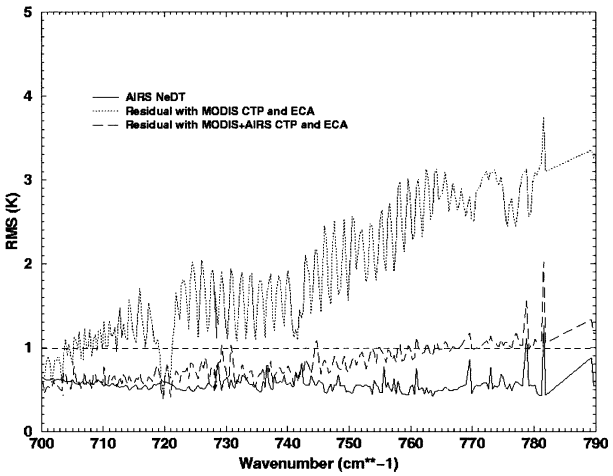

FIG. 16. The BT residual rmse with the operational MODIS cloud products and the MODIS–AIRS-retrieved cloud products, as well as the rms NeDT for AIRS granule 193 on 6 Sep 2002.

Further validation is necessary using other sources of cloud measurements such as lidar and ground observations. Retrievals in multilayer clouds still require more work; a large portion of AIRS observations appear to be in multilayer clouds, and a retrieval scheme for multilayer clouds using AIRS radiance measurements needs to be developed. Nonetheless, this preliminary work presents a strong case for the assertion that MODIS–AIRS cloud property retrievals will produce improved results over those achieved by either system alone.

Acknowledgments. The authors thank Anthony J. Schreiner for producing the 10-km GOES sounder CTP products and Richard A. Frey for numerous discussions on the MODIS CTP cloud product. The AIRS group at the University of Maryland, Baltimore County, developed and provided SARTA for the AIRS radiance calculation. This research was supported by the HES/ABI program through NOAA Grant NA07 EC00676 and by the MODIS science program through NASA Grant NAS5-31367. The views, opinions, and findings contained in this report are those of the author(s) and should not be construed as an official National Oceanic and Atmospheric Administration or U.S. government position, policy, or decision.

REFERENCES

Ackerman, S. A., K. I. Strabala, W. P. Menzel, R. A. Frey, C. C. Moeller, and L. E. Gumley, 1998: Determination of clear sky from clouds with MODIS. *J. Geophys. Res.,* **103** (D24), 32 141–32 157.

Antonelli, P., 2001: Principal component analysis: A tool for processing hyperspectral infrared data. Ph.D. thesis, University of Wisconsin—Madison. [Available from University of Wisconsin—Madison, 1225 West Dayton Street, Madison, WI 53706.]

Aumann, H. H., and Coauthors, 2003: AIRS/AMSU/HSB on the *Aqua* mission: Design, science objectives, data products, and processing systems. *IEEE Trans. Geosci. Remote Sens.,* **41,** 253–264.

Baum, B. A., and B. A. Wielicki, 1994: Cirrus cloud retrieval using infrared sounder data: Multilevel cloud errors. *J. Appl. Meteor.,* **33,** 107–117.

Bayler, G. M., R. M. Aune, and W. H. Raymond, 2000: NWP cloud initialization using GOES sounder data and improved modeling of nonprecipitating clouds. *Mon. Wea. Rev.,* **128,** 3911–3920.

Chahine, M. T., 1974: Remote sounding of cloudy atmospheres: I. The single layer cloud. *J. Atmos. Sci.,* **31,** 233–243.

Chung, S., S. A. Ackerman, P. F. van Delst, and W. P. Menzel, 2000: Calculation and interferometer measurements of ice cloud characteristics. *J. Appl. Meteor.,* **39,** 634–644.

Diak, G. R., M. C. Anderson, W. L. Bland, J. M. Norman, J. M. Mecikalski, and R. A. Aune, 1998: Agricultural management decision aids driven by real-time satellite data. *Bull. Amer. Meteor. Soc.,* **79,** 1345–1355.

Eyre, J. R., 1989: Inversion of cloudy satellite sounding radiances by nonlinear optimal estimation I: Theory and simulation. *Quart. J. Roy. Meteor. Soc.,* **115,** 1001–1026.

——, and W. P. Menzel, 1989: Retrieval of cloud parameters from satellite sounder data: A simulation study. *J. Appl. Meteor.,* **28,** 267–275.

Frey, R. A., B. A. Baum, W. P. Menzel, S. A. Ackerman, C. C. Moeller, and J. D. Spinhirne, 1999: A comparison of cloud top heights computed from airborne lidar and MAS radiance data using CO_2 slicing. *J. Geophys. Res.,* **104,** 24 547–24 555.

Gurka, J. J., and T. J. Schmit, 2002: Recommendations on the GOES-R series from the GOES users' conferences. *Applications with Weather Satellites*, W. P. Menzel et al., Eds., International Society for Optical Engineering (SPIE Proceedings Vol. 4895), 95–102.

Hannon, S., L. L. Strow, and W. W. McMillan, 1996: Atmospheric infrared fast transmittance models: A comparison of two approaches. *Optical Spectroscopic Techniques and Instrumentation for Atmospheric and Space Research II*. P. B. Hays and J. Wang, Eds., International Society for Optical Engineering (SPIE Proceedings Vol. 2830), 94–105.

Huang, H. L., W. L. Smith, J. Li, P. Antonelli, X. Wu, R. O. Knuteson, B. Huang, and B. J. Osborne, 2004: Minimum local emissivity variance retrieval of cloud altitude and effective spectral emissivity—simulation and initial verification. *J. Appl. Meteor.,* **43,** 795–809.

Isaacs, R. G., R. N. Hoffman and L. D. Kaplan, 1986: Satellite remote sensing of meteorological parameters for global numerical weather prediction. *Rev. Geophys.,* **24,** 701–743.

Kim, D. S., and S. G. Benjamin, 2000: Assimilation of cloud-top pressure derived from GOES sounder data into MAPS/RUC. Preprints, *10th Conf. on Satellite Meteorology and Oceanography*, Long Beach, CA, Amer. Meteor. Soc., 110–113.

King, M. D., and Coauthors, 2003: Cloud and aerosol properties, precipitable water, and profiles of temperature and water vapor from MODIS. *IEEE Trans. Geosci. Remote Sens.,* **41,** 442–458.

Li, J., W. P. Menzel, and A. J. Schreiner, 2001: Variational retrieval of cloud parameters from GOES sounder longwave cloudy radiance measurements. *J. Appl. Meteor.,* **40,** 312–330.

——, ——, Z. Yang, R. A. Frey, and S. A. Ackerman, 2003: High-spatial-resolution surface and cloud-type classification from MODIS multispectral band measurements. *J. Appl. Meteor.,* **42,** 204–226.

——, ——, F. Sun, T. J. Schmit, and J. Gurka, 2004: AIRS subpixel cloud characterization using MODIS cloud products. *J. Appl. Meteor.,* **43,** 1083–1094.

Lonnqvist, L., 1995: Experiences with a novel single-lens cloud height lidar. Preprints, *Ninth Symp. on Meteorological Observations and Instrumentation,* Charlotte, NC, Amer. Meteor. Soc., 106–109.

Menzel, W. P., and J. F. W. Purdom, 1994: Introducing GOES-I: The first of a new generation of geostationary operational environmental satellites. *Bull. Amer. Meteor. Soc.,* **75,** 757–781.

——, W. L. Smith, and T. R. Stewart, 1983: Improved cloud motion wind vector and altitude assignment using VAS. *J. Climate Appl. Meteor.*, **22,** 377–384.

——, D. P. Wylie, and K. I. Strabala, 1992: Seasonal and diurnal changes in cirrus clouds as seen in four years of observations with VAS. *J. Appl. Meteor.*, **31,** 370–385.

Platnick, S., M. D. King, S. A. Ackerman, W. P. Menzel, B. A. Baum, J. C. Riedi, and R. A. Frey, 2003: The MODIS cloud products: Algorithms and examples from *Terra*. *IEEE Trans. Geosci. Remote Sens.*, **41,** 459–473.

Rodgers, C. D., 1976: Retrieval of atmospheric temperature and composition from remote measurements of thermal radiation. *Rev. Geophys. Space Phys.*, **14,** 609–624.

Schmit, T. J., J. Li, and W. P. Menzel, 2002: Advanced Baseline Imager (ABI) for future Geostationary Operational Environmental Satellites (GOES-R and beyond). *Applications with Weather Satellites*. W. P. Menzel et al., Eds., International Society for Optical Engineering (SPIE Proceedings Vol. 4895), 111–122.

Schreiner, A. J., D. A. Unger, W. P. Menzel, G. P. Ellrod, K. I. Strabala, and J. L. Pellet, 1993: A comparison of ground and satellite observations of cloud cover. *Bull. Amer. Meteor. Soc.*, **74,** 1851–1861.

——, T. J. Schmit, and W. P. Menzel, 2001: Observations and trends of clouds based on GOES sounder data. *J. Geophys. Res.*, **106D,** 20 349–20 363.

Seemann, S. W., J. Li, W. Paul Menzel, and L. E. Gumley, 2003: Operational retrieval of atmospheric temperature, moisture, and ozone from MODIS infrared radiances. *J. Appl. Meteor.*, **42,** 1072–1091.

Smith, W. L., and C. M. R. Platt, 1978: Comparison of satellite-deduced cloud heights with indications from radiosonde and ground-based laser measurements. *J. Appl. Meteor.*, **17,** 1796–1802.

——, and R. A. Frey, 1990: On cloud altitude determinations from high resolution interferometer sounder (HIS) observations. *J. Appl. Meteor.*, **29,** 658–662.

——, H. M. Woolf, P. G. Abel, C. M. Hayden, M. Chalfant, and N. Grody, 1974: *Nimbus-5* sounder data processing system. Part I: Measurement characteristics and data reduction procedures. NOAA Tech. Memo. NESS 57, 99 pp.

——, ——, C. M. Hayden, D. C. Wark, and L. M. McMillin, 1979: TIROS-N operational vertical sounder. *Bull. Amer. Meteor. Soc.*, **60,** 1177–1187.

Stephens, G. L., and P. J. Webster, 1981: Clouds and climate: Sensitivity of simple systems. *J. Atmos. Sci.*, **38,** 235–247.

——, S. C. Tsay, J. P. W. Stackhouse, and P. Flatau, 1990: The relevance of the microphysical and radiative properties of cirrus clouds to climate and climatic feedback. *J. Atmos. Sci.*, **47,** 1742–1753.

Strow, L. L., S. E. Hannon, S. DeSouza-Machado, H. Motteler, and D. Tobin, 2003: An overview of the AIRS radiative transfer model. *IEEE Trans. Geosci. Remote Sens.*, **41,** 303–313.

Susskind, J., D. Reuter, and M. T. Chahine, 1987: Cloud fields retrieved from analysis of HIRS2/MSU sounding data. *J. Geophys. Res.*, **92,** 4035–4050.

——, C. D. Barnet, and J. Blaisdell, 2003: Retrieval of atmospheric and surface parameters from AIRS/AMSU/HSB data in the presence of clouds. *IEEE Trans. Geosci. Remote Sens.*, **41,** 390–409.

Wei, H., P. Yang, J. Li, B. A. Baum, A. Huang, S. Platnick, and Y. X. Hu, 2004: Retrieval of ice cloud optical thickness from Atmospheric Infrared Sounder (AIRS) measurements. *IEEE Trans. Geosci. Remote Sens.*, in press.

Wielicki, B. A., and J. A. Coakley Jr., 1981: Cloud retrieval using infrared sounder data: Error analysis. *J. Appl. Meteor.*, **20,** 157–169.

Wylie, D. P., and W. P. Menzel, 1989: Two years of cloud cover statistics using VAS. *J. Climate*, **2,** 380–392.

Yang, P., B. C. Gao, B. A. Baum, Y. X. Hu, W. J. Wiscombe, S. C. Tsay, D. M. Winker, and S. L. Nasiri, 2001: Radiative properties of cirrus clouds in the infrared (8–13 μm) spectral region. *J. Quant. Spectrosc. Radiat. Transfer*, **70,** 473–504.

——, B. A. Baum, A. J. Heymsfield, Y. X. Hu, H.-L. Huang, S.-Chee Tsay, and S. Ackerman, 2003: Single-scattering properties of droxtals. *J. Quant. Spectrosc. Radiat. Transfer*, **79–80,** 1159–1169.